ISSN 0020-1685, Inorganic Materials, 2011, Vol. 47, No. 1, pp. 45–50. © Pleiades Publishing, Ltd., 2011.
Original Russian Text © I.Sh. Trakhtenberg, A.P. Rubshtein, E.G. Volkova, S.A. Petrova, A.Ya. Fishman, R.G. Zakharov, V.B. Vykhodets, T.E. Kurennykh, 2011, published in Neorganicheskie Materialy, 2011, Vol. 47, No. 1, pp. 51–56.

Effect of Mechanical Activation on the Morphology and Structure of Hydroxyapatite

I. Sh. Trakhtenberg[a], A. P. Rubshtein[a], E. G. Volkova[a], S. A. Petrova[b], A. Ya. Fishman[b], R. G. Zakharov[b], V. B. Vykhodets[a], and T. E. Kurennykh[a]

[a] *Institute of Metal Physics, Ural Division, Russian Academy of Sciences, ul. S. Kovalevskoi 18, Yekaterinburg, 620041 Russia*
[b] *Institute of Metallurgy, Ural Division, Russian Academy of Sciences, ul. Amundsena 101, Yekaterinburg, 620016 Russia*

Received December 2, 2009; in final form, April 26, 2010

Abstract—We have studied the effect of grinding in planetary mills on the phase composition, morphology, and water content of hydroxyapatite powder. The results indicate that milling for even relatively short times, which reduces the average particle size by a factor of 2, causes the monetite present in the unmilled powder to disappear and reduces the crystallite size of the hydroxyapatite. The fraction of nanoparticles in the powder is then 98% and remains constant during further milling. Milling for longer times leads to hydroxyapatite amorphization. For an average size of large particles $R \geq 1$ μm, the surface area of the particles per unit volume, E (cm^{-1}), is determined only by R ($E \sim 1/R$).

DOI: 10.1134/S0020168510121052

INTRODUCTION

In recent years, there has been great interest in bioactive bone implant materials, motivated by the search for the most effective, biodegradable implant material, capable of initiating bone regeneration in the human body and being replaced by bone tissue [1, 2]. Synthetic materials based on calcium hydroxyapatite (HA), similar in composition to the mineral component of bone tissue, are known to improve the biomedical performance of implants for traumatic surgery, orthopedics, and dentistry. For this reason, HA powders are used not only to produce solid ceramic materials but also as additives to bone substitute materials [3, 4]. In particular, as shown by Rubshtein et al. [5], the incorporation of HA particles into a porous titanium matrix has an advantageous effect on the quality of the bone tissue forming in the pores of the implant.

This work deals with the problem of improving the performance characteristics of powder HA for use as a bioactive material in metallic matrices. A key issue is to reduce the particle size of HA (to increase the particle surface-to-volume ratio). This can be achieved by mechanical activation (milling), which is expected not only to enhance the bioactivity of the powder but also to accelerate the resorption process in pores of metallic matrices.

The objective of this work was to prepare HA nanoparticles and investigate their main morphological and structural characteristics, because the processes accompanying mechanical activation may not only reduce the particle size of HA but also modify its structure, give rise to dehydration or hydration, produce impurity phases, etc.

EXPERIMENTAL

The starting material used was modified calcium hydroxyapatite powder manufactured by ZAO NPP Biomed. This material is widely employed in medical applications. The powder was ground in a FRITSCH planetary mill (acceleration, 9 *g*; zirconia vessels and grinding media) and an AGO2 high-energy ball mill (acceleration, 40–60 *g*; steel vessels and grinding media) [6–9]. After the vessels and balls were coated with HA, a 5-g sample was ground. Every 30 s, the mill was shut off, according to the procedure described by Zyryanov et al. [7]. The background temperature was no higher than 45°C, and Fe contamination of the powder was within 10^{-2} wt %, as determined by spectral analysis.

X-ray diffraction (XRD) measurements were performed on a D8 ADVANCE diffractometer (CuK_α radiation, β-filter, VÅNTEC-1 detector, NIST SRM 1976 intensity standard). To determine the phase composition of our samples, the lattice parameters and unit-cell volume of the phases present, the crystallite size, and microstrain, we used the DIFFRAC^{Plus} software package [10, 11].

Powder morphology was examined on a QUANTA-200 scanning electron microscope (SEM) and a JEM-200CX transmission electron microscope (TEM). Powder specimens for electron-microscopic examination were stirred in ethanol and then placed in an ultrasonic bath for 10 min. The resultant dispersion of the powder in ethanol was applied to a metallic substrate or carbon film supported on a copper grid for SEM or TEM examination, respectively. Preliminary studies showed that sonication had no effect on the morphology or structure of HA particles.

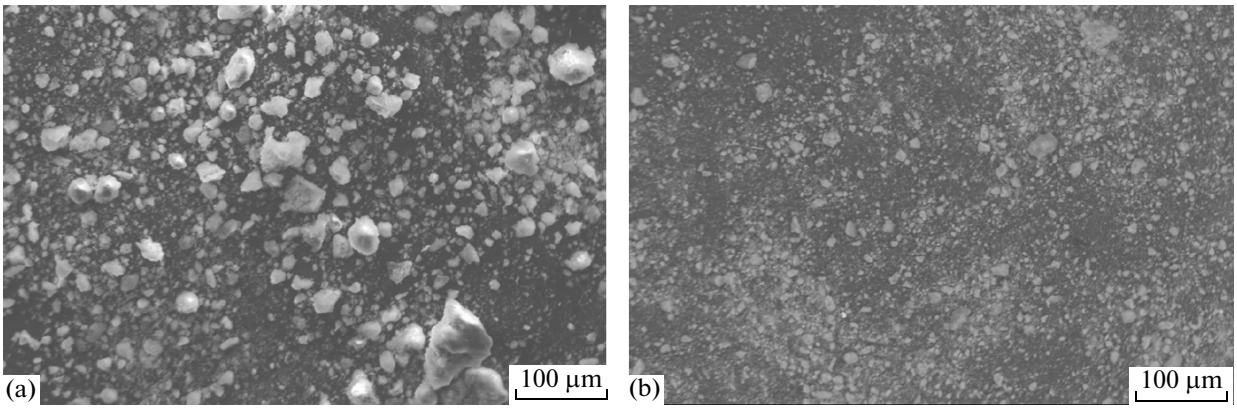

Fig. 1. SEM images of HA powder (a) before and (b) after milling for 10 min.

To determine sorbed water content, the unmilled powder and two milled samples (1 h in the FRITSCH mill and 10 min in the AGO2) were soaked in deuterated water (99.8%) for 1.5 h and then dried at 120°C for 1.5 h. The deuterium concentration in the powder was measured using a nuclear physical setup built around an EG-2M Van de Graaff electrostatic accelerator. We used the 2 ^{2}H(d, p)^{3}H nuclear reaction in a 650-keV beam.

RESULTS AND DISCUSSION

SEM examination showed that the unmilled powder consisted mainly of rather large particles. Their average size R in the range ≥2.0 μm (determined with a ±10% accuracy from the number of particles intersected by seven arbitrary lines in an SEM micrograph) was 7 μm, and the largest particles were up to 60 μm in size. Milling for 1 h in the FRITSCH mill and for 10 min in the AGO2 had identical effects: the average particle size R was 3–4 μm, and the diameter of the largest particles dropped twofold, to 30 μm (Fig. 1). According to nuclear microanalysis data, milling increased the amount of D_2O sorbed on the surface of the particles by about a factor of 2: by a factor of 3 and 1.5 (±15%) in the FRITSCH (Fig. 2) and AGO2 mills, respectively. At the same time, milling does not reduce to a decrease in particle size because of the associated friction processes and resulting point defects. Mechanical activation is known to cause structural changes, to the point of a phase transformation [12–14]. For this reason, we paid particular attention to the phase composition and morphology of the powder obtained in the AGO2, which had a higher throughput.

According to XRD data (Fig. 3), the unmilled powder consisted of two phases: HA, $Ca_{10}(PO_4)_6(OH)_2$ (ICDD, 86-1203), and monetite, $CaHPO_4$ (ICDD, 70-1425), in the ratio 3 : 2. In the unmilled sample, the crystallite size of both phases was well below 1 μm (table). Their lattice parameters are listed in the table.

It follows from the table and Fig. 3 that milling produces marked structural and phase changes in the powder. HA reacts with monetite, and the powder becomes single-phase (monetite disappears) after just 10 min of milling. The resultant HA has a factor of 10 smaller crystallite size and reduced lattice parameters and microstrain. The disappearance of monetite upon mechanical activation fits well with the experimentally observed trend that, with decreasing particle size, the phase with the lowest surface energy (with a more closely packed structure) becomes more energetically favorable [13].

Additional information, in particular about the particle morphology, can be provided by TEM. The unmilled powder consisted of elongated particles 10–40 nm in width and an order of magnitude larger in length (Fig. 4). The particles form large (~500 nm) agglomerates. In addition, there are film structures. Milling for 10 min in the AGO2 and for 1 h in the FRITSCH mill had identical

Lattice parameters of the phases present in the powder before and after milling

Sample	τ, min	Phase	Sp. gr.	a, nm	c, nm	D, nm	ε, %
1	Unmilled	HA	$P6_3/m$ (176)	0.94605	0.68996	540	0.32
		Monetite	$P\bar{1}(2)$	0.68941	0.66536	412	0.10
2	10	HA	$P6_3/m$ (176)	0.94456	0.68883	39	0.08
3	20	HA	$P6_3/m$ (176)	0.94506	0.68884	41	0.021
4	40	HA	$P6_3/m$ (176)	0.94499	0.68893	31	0.13

Note: D is the crystallite size and ε is microstrain.

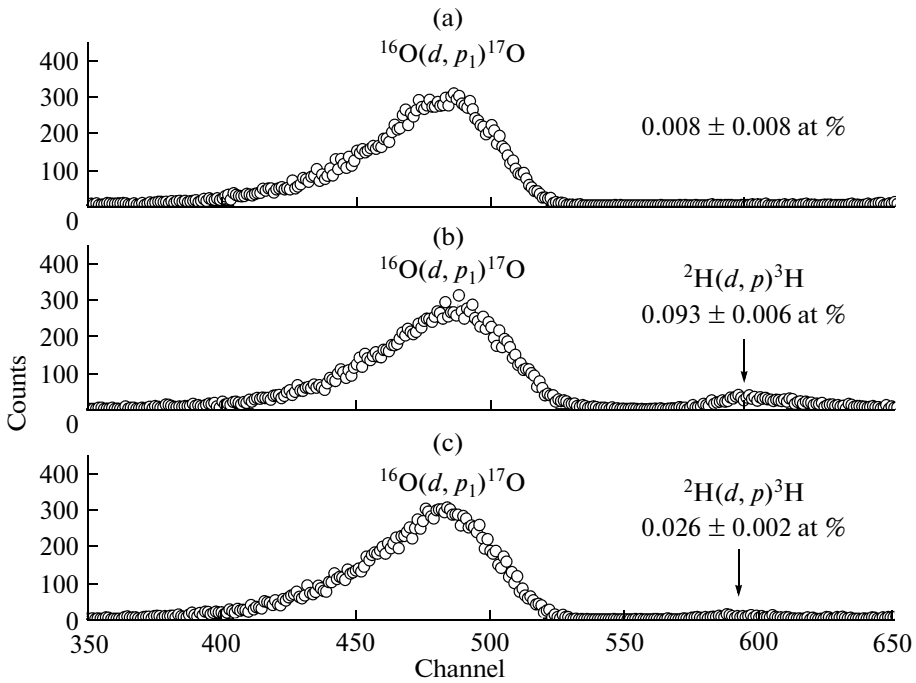

Fig. 2. Nuclear reaction spectra for HA samples: (a) unmilled, no D_2O soaking; (b) milled for 1 h in the FRITSCH mill and soaked in D_2O; (c) unmilled, soaked in D_2O.

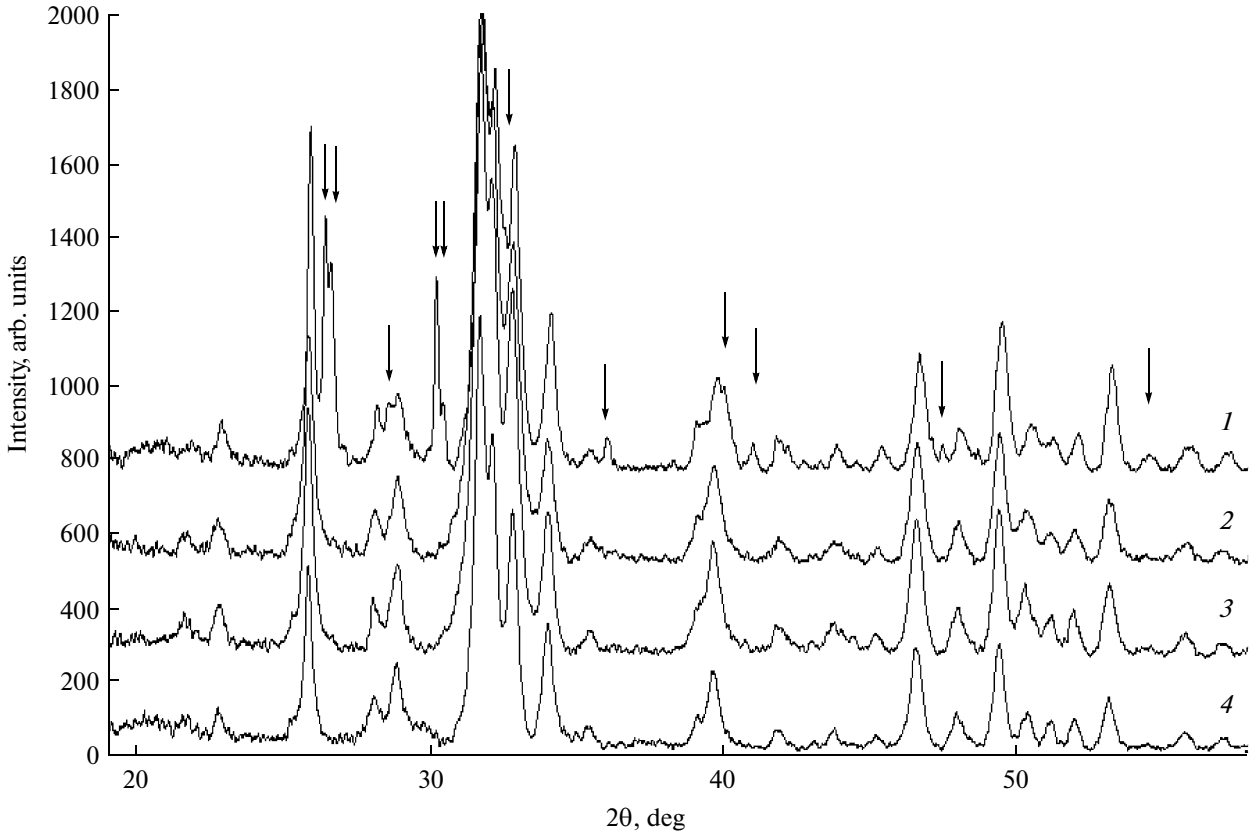

Fig. 3. XRD patterns of the (*1*) unmilled and (*2–4*) milled HA samples. The total time of milling in the AGO2 is specified in the table. The arrows show the positions of the strongest reflections from monetite.

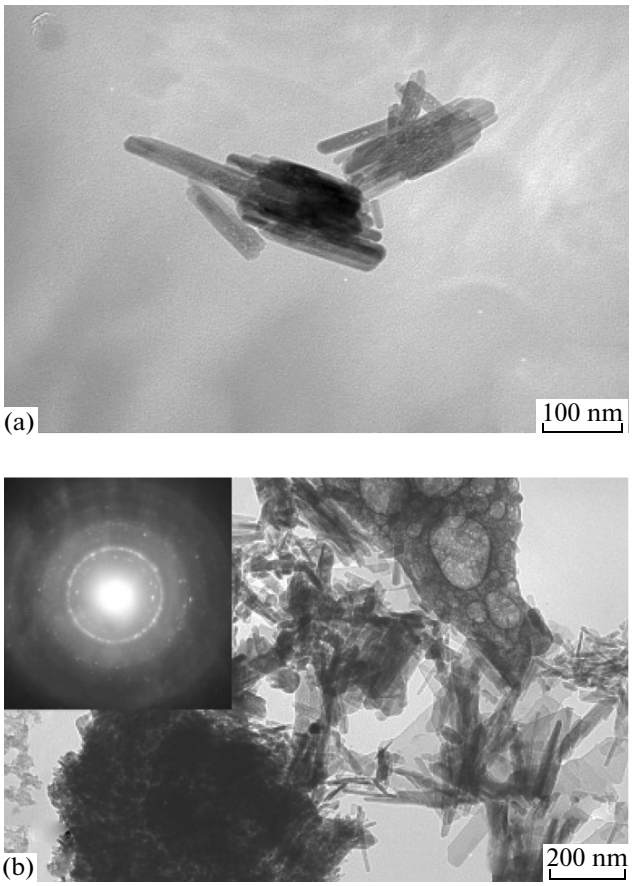

Fig. 4. TEM images of the unmilled HA powder: (a) individual particles; (b) general view showing individual particles, particle accumulations, and film structures. Inset: selected area electron diffraction pattern.

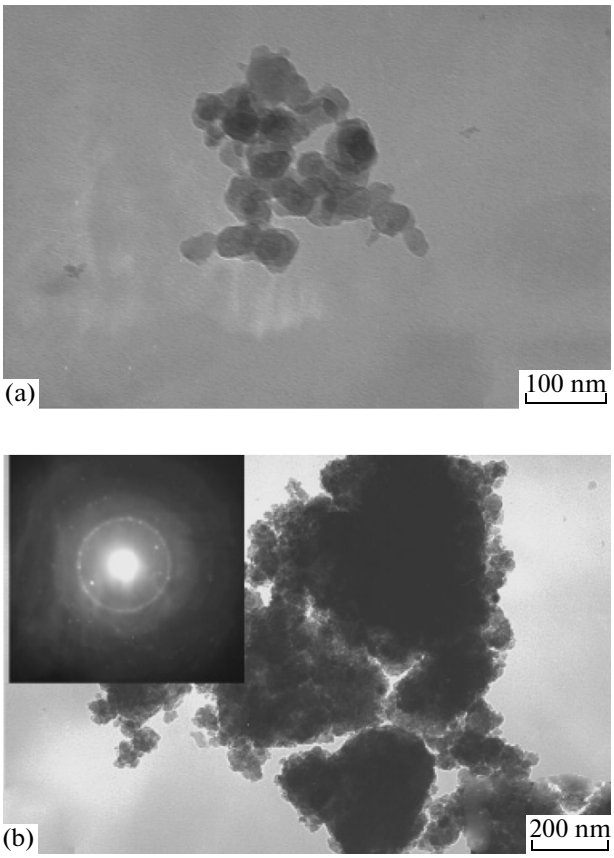

Fig. 5. TEM images of the HA powder after milling for 10 min. Inset: selected area electron diffraction pattern.

effects (Fig. 5a): small elongated particles typical of the unmilled powder were missing, and we observed rounded particles 10–130 nm in size and agglomerates 500 nm and more in size. Further milling produced no significant changes in the morphology of the fine particles, but milling for 40 min increased the amount of film structures and caused amorphization (Fig. 6).

We evaluated the fraction of particles in the size range 10–40 nm relative to the total number of particles (taking averages over five TEM images). The most drastic changes in the particle size distribution were observed in the initial stages of milling: the fraction of particles less than 50 nm in radius r increased from 25 to 98% and subsequently varied little. Clearly, this is the result of a dynamic equilibrium between two processes: the formation of nanoparticles (resulting from friction between micron-sized parent particles) and agglomeration of fine particles.

The mechanism of powder disintegration and attrition is no doubt related to the crystal structure of HA. HA has a hexagonal lattice, with typical slip on the {0001} basal planes, $\{1\bar{1}00\}$ prism, $\{\{1\bar{1}01\}\}$ first-order pyramid, and $\{11\bar{2}2\}$ second-order pyramid. The c parameter of HA is smaller than its a parameter, and the main slip planes for defects are the $\{1\bar{1}00\}$ prism faces. For this reason, the narrow, long HA particles present in the unmilled powder readily break down along these planes and become rounded during mechanical activation. With increasing milling time and decreasing particle size, the {0001} basal planes become the main slip planes, with a tendency toward the formation of film structures.

It is of interest to analyze the effectiveness of mechanical activation in terms of practical applications of HA. Useful interactions of HA particles with biological tissues (initiation of bone tissue ingrowth and phosphorus and calcium delivery for this process) take place on the particle surface. The rate of particle–medium interaction (transition of the components of the particle material to the medium) is determined by the particle surface-to-volume ratio, S_i/V_i. We use $E_i = S_i/V_i$ to quantify the ability of a particle to supply the substances present in it to a medium containing bone marrow cells. Moderate-rate milling, resulting in the formation of single-phase HA in which 98% of the particles are three orders of magnitude smaller than

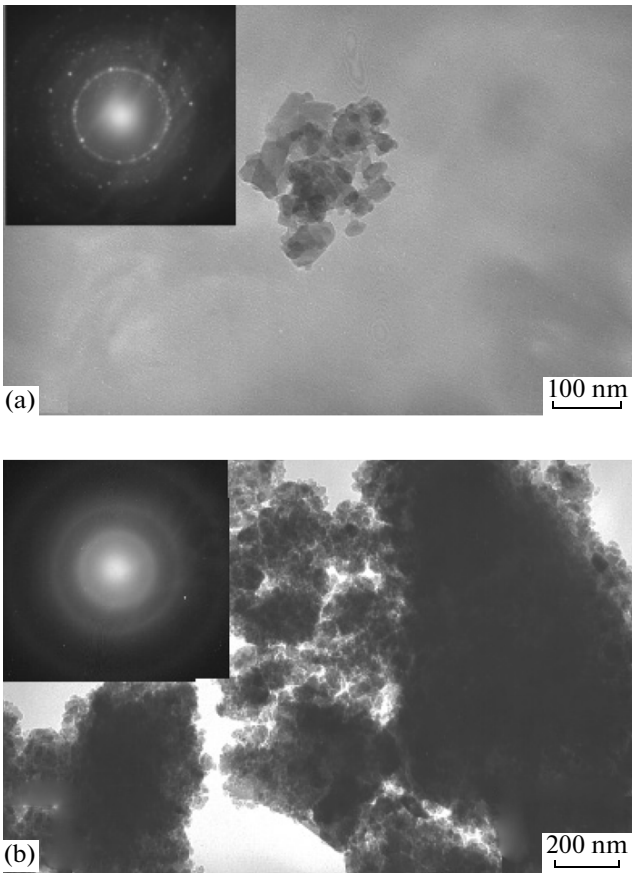

Fig. 6. TEM images of the HA powder after milling for 40 min. Insets: selected area electron diffraction patterns.

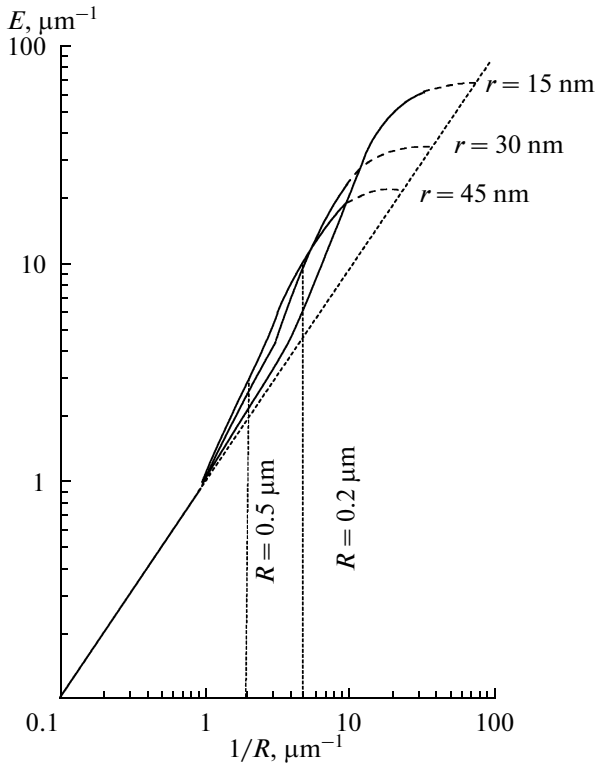

Fig. 7. Log–log plots of the ratio of the total surface area of particles to their total volume, E, against the inverse of the average radius of the largest particles, R, for powder in which 98% of the particles have a radius $r < 50$ nm.

the particles in the unmilled powder, is expected to be favorable for accelerated growth of bone tissue at the beginning of the postimplantation period. At the same time, the efficacy of HA powder should be quantified by the ratio of the total surface area of the particles to their total volume, $E = \sum S_i / \sum V_i$. To make a rough estimate, we neglect the form factor, take $S_i \sim R_i^2$, and $V_i \sim R_i^3$, and divide the ensemble of N particles into two groups with average particle sizes R and r and fractions of particles α and β, respectively. We obtain

$$E = \left(N\alpha R^2 + N\beta r^2\right) \Big/ \left(N\alpha R^3 + N\beta r^3\right)$$
$$= \left[1 + (\beta/\alpha)\left(r^2/R^2\right)\right] \Big/ \left[R + r(\beta/\alpha)\left(r^2/R^2\right)\right].$$

Figure 7 shows log–log plots of E against $1/R$ in the range $r \le R \le 10$ μm for three hypothetical average values $r \le 50$ nm and an experimentally determined ratio $\beta/\alpha = 49$.

It can be seen from Fig. 7 that, when the average particle size of the unmilled powder lies in the micron range ($R \ge 1$ μm), the fine particles ($r \le 50$ nm), which result from powder disintegration through attrition, have no effect on $E \sim 1/R$. At the same time, further milling does not eliminate large particles ($R \ne r$) because it is accompanied by particle agglomeration. According to TEM results (Figs. 4–6), the average agglomerate size R ranges from 200 to 500 nm. This implies (Fig. 7) that prolonged milling can increase E by no more than two orders of magnitude (20 μm$^{-1} \le E \le$ 90 μm^{-1}). In addition, the efficacy of HA powder is significantly influenced by the size distribution of such particles (which is illustrated in Fig. 7 by varying the average value r for particles with $r <$ 50 nm).

CONCLUSIONS

Mechanical activation of two-phase (HA + monetite) powder leads to the formation of single-phase HA even in the initial stages of milling (1 h in the FRITSCH mill and 10 min in the AGO2). After milling, the amount of fine particles ($r < 50$ nm) exceeds that of larger particles by about two orders of magnitude. With increasing milling time, the fine particles become rounded and cleave along the closest-packed atomic planes, leading to the growth of film structures. Despite the reduction in the average size R of the parent particles, the fraction of fine particles ($r < 50$ nm) remains constant at 98% because of their agglomeration. When R lies in the micron range, the surface area of the powder per unit volume is determined

only by large particles and varies as ~1/*R*. Despite the constant fraction of nanoparticles, the structure of the HA particles varies with milling time (milling for 40 min in the AGO2) and the material experiences amorphization.

Therefore, given that prolonged milling may reduce the amount of water of crystallization (which is undesirable), two mechanical activation procedures can be recommended for testing their biomedical utility in vitro and in vivo. These are the initial stages of milling, when the particle size decreases by less than ten times, but the powder becomes single-phase and contains 98% nanoparticles, and the crystal structure of the HA undergoes only slight changes, and prolonged milling, which drastically reduces the particle size (increases the surface area of the particles per unit volume), but the powder also contains 98% nanoparticles and larger agglomerates, and the HA experiences amorphization.

REFERENCES

1. Barinov, S.M. and Komlev, V.S., *Biokeramika na osnove fosfatov kal'tsiya* (Calcium Phosphate Based Bioceramics), Moscow: Nauka, 2005.
2. Hench, L.L., Bioceramics: From Concept to Clinic, *J. Am. Ceram. Soc.,* 1991, vol. 74, no. 7, pp. 1487–1510.
3. Jarcho, M., Calcium Phosphate Ceramics As Hard Tissue Prosthetics, *Clin. Orthop. Relat. Res.,* 1981, vol. 157, pp. 259–287.
4. Zakharov, N.A., Ezhova, Zh.A., Koval', E.M., et al., Hydroxyapatite–Carboxymethyl Cellulose Nanocomposite Biomaterial, *Neorg. Mater.,* 2005, vol. 41, no. 5, pp. 592–599 [*Inorg. Mater.* (Engl. Transl.), vol. 41, no. 5, pp. 509–515].
5. Rubshtein, A.P., Trakhtenberg, I.Sh., Makarova, E.B., and Osipenko, A.V., Effect of Nanocomposite Nitrogen-Containing Carbon Films on Bone Tissue Formation in a Porous Hydroxyapatite-Containing Titanium Implant, *Perspekt. Mater.,* 2009, no. 3, pp. 52–56.
6. Zyryanov, V.V. and Lapina, O.B., Mechanochemical Synthesis and Structure of New Phases in the Pb–V–O System, *Neorg. Mater.,* 2001, vol. 37, no. 3, pp. 331–337 [*Inorg. Mater.* (Engl. Transl.), vol. 37, no. 3, pp. 264–270].
7. Zyryanov, V.V., Sysoev, V.F., Boldyrev, V.V., and Korosteleva, T.V., USSR Inventor's Certificate no. 1375328, *Byull. Izobret.,* 1988, no. 7, p. 39.
8. Osipyan, V.G., Savchenko, L.M., Avakumov, E.G., and Uvarov, N.F., *Mekhanokhimicheskii sintez v neorganicheskoi khimii* (Mechanochemical Synthesis in Inorganic Chemistry), Novosibirsk: Nauka, 1991, pp. 83–101.
9. Lazure, S., Vernochet, Ch., Vannier, R.N., et al., Composition Dependence of Oxide Anion Conduction in the BIMEVOX Family, *Solid State Ionics,* 1996, vol. 90, pp. 117–123.
10. Diffrac^{Plus}*: Eva Bruker AXS GmbH, Ostliche,* Rheinbruckenstraße 50, D-76187, Karlsruhe: Germany, 2007.
11. Diffrac^{Plus}*: Topas Bruker AXS GmbH, Ostliche,* Rheinbruckenstraße 50, D-76187, Karlsruhe: Germany, 2006.
12. Andrievskii, R.A., *Poroshkovoe materialovedenie* (Powder Materials Technology), Moscow: Metallurgiya, 1991.
13. Gorbacheva, T.B., *Rentgenografiya tverdykh splavov* (X-ray Diffraction of Hard Alloys), Moscow: Metallurgiya, 1985.
14. Morokhov, I.D., Trusov, L.I., and Lapovok, V.N., *Fizicheskie yavleniya v ul'tradispersnykh sredakh* (Physical Phenomena in Highly Dispersed Media), Moscow: Energoatomizdat, 1984.